# NOAA Technical Report NESDIS 133

# Methodology and Information Content of the NOAA/NESDIS Operational Channel Selection for the Cross-Track Infrared Sounder (CrIS)

Washington, D.C.
August 2011

**U.S. DEPARTMENT OF COMMERCE**
**National Oceanic and Atmospheric Administration**
National Environmental Satellite, Data, and Information Service

**NOAA TECHNICAL REPORTS**

**National Environmental Satellite, Data, and Information Service**

**The National Environmental Satellite, Data, and Information Service (NESDIS) manages the Nation's civil Earth-observing satellite systems, as well as global national data bases for meteorology, oceanography, geophysics, and solar-terrestrial sciences. From these sources, it develops and disseminates environmental data and information products critical to the protection of life and property, national defense, the national economy, energy development and distribution, global food supplies, and the development of natural resources.**

**Publication in the NOAA Technical Report series does not preclude later publication in scientific journals in expanded or modified form. The NESDIS series of NOAA Technical Reports is a continuation of the former NESS and EDIS series of NOAA Technical Reports and the NESC and EDS series of Environmental Science Services Administration (ESSA) Technical Reports.**

**An electronic copy of this report may be obtained at http://www.star.nesdis.noaa.gov/star/smcd_pub.php**

**A limited number of copies of earlier reports are available by contacting Susan Devine, NOAA/NESDIS, E/RA, 5200 Auth Road, Room 701, Camp Springs, Maryland 20746, (301) 763-8127 x136.**

**A partial listing of more recent reports appears below:**

**NESDIS 102** **NOAA Operational Sounding Products From Advanced-TOVS Polar Orbiting Environmental Satellites. Anthony L. Reale, August 2001.**

**NESDIS 103** **GOES-11 Imager and Sounder Radiance and Product Validations for the GOES-11 Science Test. Jaime M. Daniels and Timothy J. Schmit, August 2001.**

**NESDIS 104** **Summary of the NOAA/NESDIS Workshop on Development of a Coordinated Coral Reef Research and Monitoring Program. Jill E. Meyer and H. Lee Dantzler, August 2001.**

**NESDIS 105** **Validation of SSM/I and AMSU Derived Tropical Rainfall Potential (TRaP) During the 2001 Atlantic Hurricane Season. Ralph Ferraro, Paul Pellegrino, Sheldon Kusselson, Michael Turk, and Stan Kidder, August 2002.**

**NESDIS 106** **Calibration of the Advanced Microwave Sounding Unit-A Radiometers for NOAA-N and NOAA-N=. Tsan Mo, September 2002.**

**NESDIS 107** **NOAA Operational Sounding Products for Advanced-TOVS: 2002. Anthony L. Reale, Michael W. Chalfant, Americo S. Allegrino, Franklin H. Tilley, Michael P. Ferguson, and Michael E. Pettey, December 2002.**

**NESDIS 108** **Analytic Formulas for the Aliasing of Sea Level Sampled by a Single Exact-Repeat Altimetric Satellite or a Coordinated Constellation of Satellites. Chang-Kou Tai, November 2002.**

**NESDIS 109** **Description of the System to Nowcast Salinity, Temperature and Sea nettle (*Chrysaora quinquecirrha*) Presence in Chesapeake Bay Using the Curvilinear Hydrodynamics in 3-Dimensions (CH3D) Model. Zhen Li, Thomas F. Gross, and Christopher W. Brown, December 2002.**

**NESDIS 110** **An Algorithm for Correction of Navigation Errors in AMSU-A Data. Seiichiro Kigawa and Michael P. Weinreb, December 2002.**

NOAA Technical Report NESDIS 133

# Methodology and Information Content of the NOAA/NESDIS Operational Channel Selection for the Cross-Track Infrared Sounder (CrIS)

Antonia Gambacorta[1] and Chris Barnet[2]

1. Dell Perot Systems
   8270 Willow Oaks Corp Dr #300
   Fairfax, VA 22031

2. NOAA/NESDIS/STAR
   5200 Auth Road
   Camp Springs, MD 20746

Washington, DC
August 2011

**U.S. DEPARTMENT OF COMMERCE**
Gary Locke, Secretary

**National Oceanic and Atmospheric Administration**
Dr. Jane Lubchenco, Under Secretary of Commerce for Oceans and Atmosphere
and NOAA Administrator

**National Environmental Satellite, Data, and Information Service**
Mary Kicza, Assistant Administrator

# Methodology and information content of the NOAA NESDIS operational channel selection for the Cross-Track Infrared Sounder (CrIS)

A. Gambacorta and C. D. Barnet

NOAA NESDIS STAR, Camp Springs, MD, USA
(corresponding author: antonia.gambacorta@noaa.gov)

NOAA NESDIS Technical Report n.133

August 25th, 2011

**Abstract**

We describe the NOAA NESDIS channel selection methodology for the Cross-track Infrared Sounder, scheduled to be launched in October 2011 and to become operational in 2012. We describe the main spectral characteristics and we discuss the information content of the final channel subset that will be distributed to the scientific community for operational data assimilation and retrieval applications. This channel selection is composed of 399 channels and its information content is shown to retain most of the total atmospheric variability contained in the original 1305 channel spectrum, up to instrumental noise.

## 1 Introduction

The Cross-track Infrared Sounder (CrIS) and the Advanced Technology Microwave Sounder (ATMS) are planned to be flown aboard the Joint Polar Satellite System (JPSS) and form the next generation of atmospheric operational sounders [4]. The CrIS instrument is a Fourier transform spectrometer with a total of 1305 infrared sounding channels spread over 3 bands covering the longwave (655-1095 $cm^{-1}$), midwave (1210-1750 $cm^{-1}$), and shortwave (2155-2550 $cm^{-1}$) region, with a spectral resolution of 0.625 $cm^{-1}$, 1.25 $cm^{-1}$ and 2.5 $cm^{-1}$ respectively.

Given the large yield of the expected data flow, a channel selection is required that will expedite the near real time data distribution and assimilation. Although hyper spectral data are affected by a considerable redundancy, at-

tention must be paid aimed at minimizing the loss of information during the selection procedure, such that the final retrieval quality is not deteriorated.

The purpose of this paper is to describe the NOAA/NESDIS channel selection methodology applied to the CrIS instrument and to present the main spectral characteristics of the final channel subset that will be distributed to the scientific community for near real time data assimilation and retrieval applications. This paper is divided in two parts. Section 2 provides a detailed description of the channel selection methodology. Focus of this section is an assessment of the degree of spectral purity associated to each selected channel. Section 3 and 4 assess the information content present in the selection by performing a principal component analysis and quantifying the fraction of the full spectrum atmospheric variance explained by this selection.

## 2 Channel Selection Methodology

The finite spectral resolution of the instrument does not allow for *spectral purity*. That is, in the infrared domain, the signal associated to a channel of nominal frequency $\nu$ is the result of multiple molecular roto-vibrational transitions occurring in the same spectral range of the nominal spectral resolution, $\Delta\nu$, of that channel. For a given atmospheric species of interest then, the accuracy of the retrieval and its associated error characterization, rests on the knowledge of the degree of spectral purity present in the subset of channels selected to run the retrieval step of that given species.

We employ the UMBC SARTA radiative transfer model [14] to compute a spectral sensitivity analysis of the full CrIS spectrum. We use standard US atmospheric profiles to perform brute force perturbations of temperature, water vapor and trace gases (ozone, methane, carbon dioxide, carbon monoxide, $HNO_3$, $N_2O$, and $SO_2$). We first analize the radiance response to each perturbation, $\Delta R(\nu)$, represented by the difference between the perturbed and the unperturbed radiance spectra. In this methodology, derivatives of the radiance spectrum, defined as spectral sensitivity functions $S(\nu)$, are computed by finite differencing for each perturbation $\delta X_j$, according to the equations:

$$S(\nu)\delta X_j = \frac{\partial R(X_o, \nu)}{\partial X_j}\partial X_j \approx \Delta R_j(\nu) \tag{1}$$

$$\Delta R_j(\nu) = (R(X_o + \delta X_j) - R(X_o)) \tag{2}$$

Where R is the radiance signal, $X_o$ represents the unperturbed atmospheric state, $\delta X_j$ is the perturbation associated to species j. These radiance differences indicate the sensitivity of each channel to each specific atmospheric species of interest and are used in our study as indexes of spectral purity.

Figure 1, provides an illustrative example of this sensitivity analysis, applied to the case of a mid-latitude US standard atmospheric profile. Here the different curves represent differences in brightness temperature due to a perturbation in

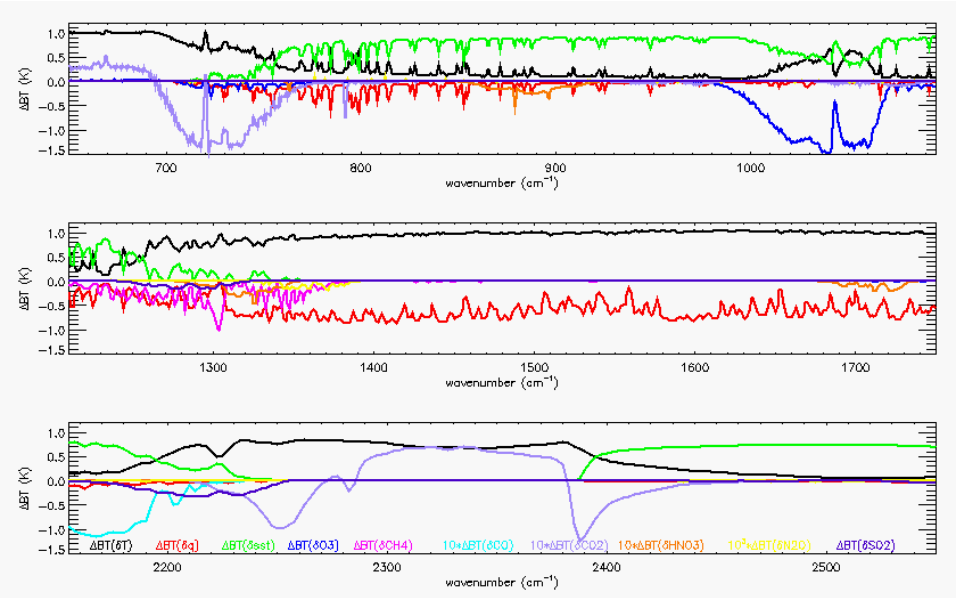


Figure 1: Sensitivity Analysis of CrIS channels. Black curve: temperature sensitivity analysis. Red curve: water vapor sensitivity analysis. Green curve: surface temperature sensitivity analysis. Blue curve: ozone sensitivity analysis. magenta curve: methane sensitivity analysis. Cyan curve: carbon monoxide sensitivity analysis. For display purposes a factor multiplier equal to 10 has been used. Light Purple: carbon dioxide sensitivity analysis. For display purposes a factor multiplier equal to 10 has been used.Oragen curve: $HNO_3$ sensitivity analysis. For display purposes a factor multiplier, FM, equal to 10 has been used. Yellow curve: $N_2O$ sensitivity analysis. For display purposes a factor multiplier equal to $10^3$ has been used. Dark Purple: $SO_2$ sensitivity analysis.

temperature (1K degree perturbation, black curve), water vapor (10% perturbation, red curve), ozone (10% perturbation, blue curve), surface temperature (1K degree perturbation, green curve), methane (2% perturbation, magenta) and carbon monoxide (1% perturbation, cyan), carbone dioxide (1% perturbation, light purple), $HNO_3$ (1% perturbation, orange), $N_2O$ (1% perturbation, yellow) and $SO_2$ (1% perturbation, dark purple).

A preliminary channel screening is computed on the basis of the sensitivity features highlighted in Figure 1. We section the spectrum into different channel subsets, each subset including channels highly sensitive to a specific atmospheric species of interest and with the lowest sensitivity to all remaining species. In doing so, for example, temperature sounding channels will be preferentially selected in the $670cm^{-1}$ and $2300cm^{-1}$ regions, where the sensitivity to temperature perturbation is high (black curve) and the intereference of other species is minimal or is well known (see ahead discussion on noise covariance).

After this preliminary screening, we closely study the properties of the vertical sensitivity functions, $S(\nu)$, associated to the selected channels. Since the shape of the sensitivity functions is influenced by temperature and pressure as well as by the vertical variation of the atmospheric species mixing ratio, the selection of channels whose sensitivity functions peak at different altitudes enables vertical sounding of the atmosphere.

The finite spectral resolution of the instrument is responsible for broadening the channel sensitivity functions into coarse vertical ranges. Channels with sharper sensitivity functions are then preferentially selected over broadly structured ones, in the attempt of maximizing the vertical resolution of the retrieval product.

In summary, the NOAA/NESDIS methodology is a phisically based procedure where channels are selected solely upon their spectral properties. Redundancy is removed by selecting channels with the highest spectral purity and whose sensitivity function structure maximizes vertical sounding coverage and resolution.

The example shown in figure 1 refers to a mid-latitude profile. We have performed this sensitivity study on multiple atmospheric test cases, representative of different atmospheric regimes (ocean/land, polar, mid-latitude and tropical regimes). The final channel selection proved uniform sensitivity features under different air mass conditions, a fundamental requirement to achieve global optimality and robustness in the retrieval applications.

The final channel selection is composed of a total of 399 channels distributed as 24 surface temperature and emissivity sounding channels, 87 temperature sounding channels, 62 water vapor, 53 ozone, 27 carbon monoxide, 54 methane, 53 carbon dioxide, 24 $N_2O$, 28 $HNO_3$ and 24 $SO_2$ sounding channels. Grey cross symbols on figures 2 indicate the location of all 1305 channels present in CrIS original spectra. Superimposed colored cross symbols indicate the 10 channel subsets forming our final channel selection. Here we have adopted the same color codes of figure 1 to indicate the different atmospheric species to which the selected channels are mainly sensitive. The full list of selected channels is given in the table 1 of the attached appendix. Here, the first column reports the channel index, the second column reports the actual channel frequency. In the third column, we have flagged each channel according to the atmospheric species of highest sensitivity, while the fourth column reports the total column spectral transmissivity of the main interfering atmospheric species (fixed composition gases, water vapor, ozone and liquid water) as an index of spectral purity.

The main spectral and noise characteristics of this channel selection are summarized in the paragraphs below.

## 2.1 Selection of temperature sounding channels

Temperature sounding requires channels sensitive to well mixed and slowly varying gases. Infrared sounders normally employ channels sensitive to carbon dioxide which has two strong fundamentals in the infrared spectrum, specifically in the $670cm^{-1}$ and $2300cm^{-1}$ regions (commonly expressed in microns as: $15\mu m$

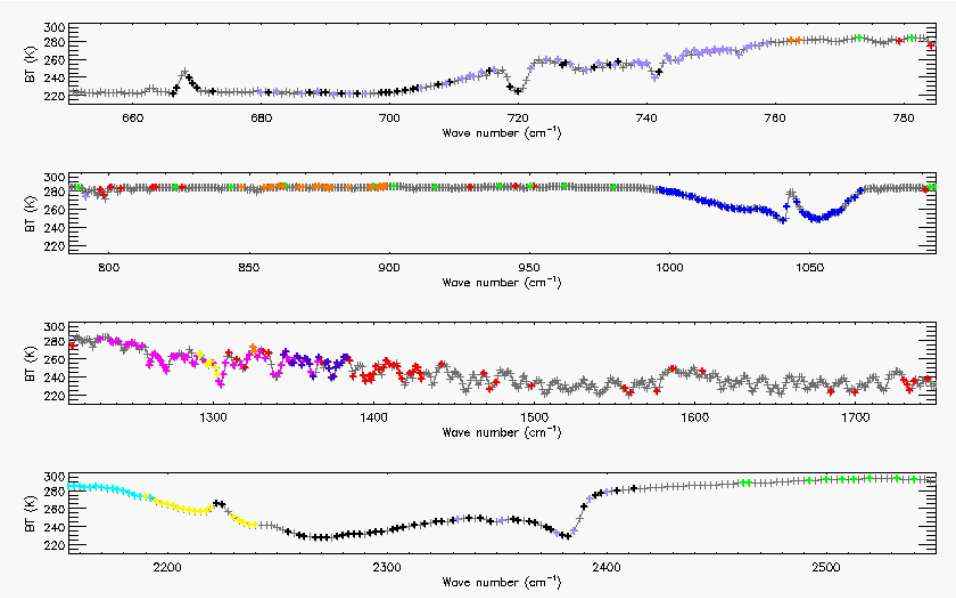


Figure 2: Final channel selection. Grey cross symbols indicate the location of all 1305 channels present in CrIS original spectra. Superimposed colored cross symbols indicate the 10 channel subsets forming our final channel selection. The final selection is composed of 24 surface temperature and emissivity sounding channels (green), 87 temperature sounding channels (black), 62 water vapor (red), 53 ozone (blue), 27 carbon monoxide (cyan), 54 methane (magenta), 53 carbon dioxide (light purple), 24 $N_2O$ (yellow), 28 $HNO_3$ (orange) and 24 $SO_2$ (dark purple) sounding channels. The total number of channels is 399.

and 4.3 $\mu m$ bands). We follow previous theoretical studies by kaplan *et al.* [10], and preferentially select channels along the wings of $CO_2$ transition lines, whose weighting functions were shown to have half the width at half peak as that of core channel weighting functions, due to the rapid increase of the absorption coefficient with pressure.

As shown in [9] the most pronounced sensitivity functions are found in the $2300cm^{-1}$ band. This is due to the rapid increase of the absorption coefficient with tropospheric temperature. Besides the higher instrumental noise, the only complication of the shortwave band is the high solar reflectivity term affecting the surface and low troposphere sounding channels on one side, and the non local thermodynamic equilibrium affecting the upper and stratospheric sensitive channels, on the other. These factors, both occurring during daily conditions, are affected by large uncertainties during forward model calculations.

The complementary $670cm^{-1}$ channels become fundamental for sounding under the conditions of partial cloudiness [2]. Long-wave channels have good sensitivity to temperature from the surface to the stratosphere, up to 1mb. The

only complication affecting this band rests in the interference of water vapor and ozone as opposed to the head band of the $2300cm^{-1}$ spectral region which instead shows low sensitivity to these two interfering species.

The temperature subset is also applicable for cloud filtering [15]. For cloud height retrievals based on $CO_2$ slicing techniques [2], only the long wave subset of this selection is used in order to avoid solar reflectance effects, as described earlier, and because of the uncertainty in the radiative properties of low cloud emissivity.

The selection of surface temperature channels requires high transmittance from all atmospheric components. A total of 24 channels have been selected in the 750 - 1100 $cm^{-1}$ and 2150 - 2540 $cm^{-1}$ window regions. Attention is required when using channels in the 1000 - 1275 $cm^{-}1$ band, due to existing difficulties in the parametrization of desert emissivity.

## 2.2 Selection of atmospheric constituent sounding channels

For atmospheric constituents, core spectral line have been favored over wing line channels in order to maximize the signal to noise ratio, with equivalent attention to spectral purity and sensitivity function sharpness properties. Complementary wing line channels have been added to the selection in the attempt of improving the vertical coverage of the channel selection sensitivity, enabling vertical profile retrievals.

## 2.3 Instrumental and Apodization Noise effects

A large effort of the selection methodology also involves a thorough scrutiny of the channel noise properties. The selection generally tends to avoid channels with high instrumental noise such as those in the shortwave region, and channels affected by poor calibration.

Careful attention must also be paid to the noise correlation of adjacent channels resulting from apodization. The expansion of an apodization function into an infinite cosine series enables the determination of the apodization noise reduction factor and spectral correlation among adjacent channels.

Apodized radiances sampled at the Nyquist sampling can be written as a $2J-1$ point running mean of the raw instrument radiances with weights, $w_k$, given by Eqn 4:

$$R_{apod}(v') = \sum_{k=-J+1}^{J-1} w_k R(v+k) \tag{3}$$

We can define the weights, $w_k$, in terms of the cosine expansion coefficients, $a_k$, as follows:

$$w_k = a_{|k|}, for k = -(J-1), ..., J-1 \tag{4}$$

The apodized noise is reduced by a factor, *f*, given by:

$$f = [\sum_{k=-J+1}^{J-1} w_k^2]^{-1/2} \tag{5}$$

and the channel correlation for a channel separated by n Nyquist channels is given by:

$$CF_n = f^2 \sum_{k=-J+1}^{J-1-n} w_k w_{k+n} \tag{6}$$

where n=1, ..., 2J-2.

CrIS radiances are apodized using a Hamming apodization function. Hamming apodization has J = 2 and $a_0 = 0.54$ and $a_1 = 0.23$, so that $w_1 = 0.23$, $w_0 = 0.54$, $w_1 = 0.23$ and $\sum(w_k) = 1$. Hamming apodization is able to reduce CrIS's noise by a factor f = 1.5862. In turn, adjacent channels are now correlated by a correlation factor $CF_1 = 62.5\%$ and alternate channels are correlated by $CF_2 = 13.3\%$. Channels separated by more then two indexes have zero correlation. In the attempt of maximizing the vertical sensitivity coverage, the proposed channel selection does contain, at times, few groups of adjacent channels. Users are advised then to pick every other third channel from the proposed selection, if in need of eliminating apodization correlation noise effects. In doing so though, attention must be paid to still retain uniform sensitivity coverage along the vertical atmospheric column.

## 2.4 Applications

The issue of spectral impurity affecting the accuracy of the retrieval product can be circumvented by exploiting the distinctive non-linearity of the radiative interference sources shown in Figures 1. During the retrieval of a given species of interest, the interference signals of undesired species (held constant at that step) can be treated as radiance error sources that can be used as off-diagonal terms of the observed radiance error covariance matrix. In doing so, the least square minimization is made insensitive to the interfering species and the inversion problem can be solved by parts. In this scheme, the perturbation on species $X_j$, from which we compute the associated error source $\Delta R_j(\nu)$, is derived from an error estimate on the geophysical species, $\delta X_j$. The corresponding computational uncertainty $\Delta R_j(\nu)$ is a finite difference expressed by Eq. 7:

$$\Delta R_j^{s,i}(v) = (R(X_o^{s,i-1} + X_j * Q_j) - R(X_o^{s,i-1})) \tag{7}$$

where $X_o$ is the current estimate of the geophysical state at a given step $s$ and iteration $i$. $\delta X_j$ is the perturbation on the $X_j$ component.

Since $\delta X_j$ is an RSS error estimate, it can be vertically cross-correlated and spectrally correlated with respect to other parameters (e.g., surface spectral emissivity error can be correlated with skin temperature). A scaling factor $Q_j$ is needed to compensate for assumed correlations in these error estimates.

During the retrieval step $s$ and iteration $i$ of a given species of interest, the off diagonal terms of the error covariance matrix will be obtained from the summation of all radiance interference terms from undesired geophysical species (held constant during that retrieval step), as in Eq. 8:

$$\Delta R(\nu, \nu') = \sum_{j=0}^{N-1} \Delta R_j^{s,i}(\nu)(\Delta R_j^{s,i}(\nu'))^T \tag{8}$$

The accuracy of the solution will strongly depend on the accuracy of the radiative transfer model used to compute these off-diagonal noise terms.

The approach described above forms the basics of the current NASA operational hyper spectral inversion algorithm for the Atmospheric InfraRed Sounder (AIRS), [15], and the NOAA/NESDIS Infrared Atmospheric Sounding Instrument (IASI), [6], whose operational channel selections were performed following the same methodology described in this paper, [7]. The same inversion scheme will be employed for the NOAA/NESDIS operational processing of CrIS data.

On the other hand, this channel selection is also suitable for alternative 1-DVAR-like inversion techniques, which can resort to the interference of multiple species affecting a given channel, as described by the curves of Figure 1, to simultaneously solve for multiple species of interest. At present, the National Center for Environmental Prediction (NCEP) employes a 1-DVAR inversion technique to operationally process the aforementioned AIRS and IASI channel selections, along with the CrIS channel selection discussed in this paper.

# 3 Information content analysis

## 3.1 Singular value decomposition analysis (SVD)

We have used a sub-sample of a global CrIS proxy data from October 19 2007 [1] where we have considered only the first two scan lines of each granule, for a total of$\tilde{1}$4000 radiance spectra, uniformly including ocean/land/day/night cases. We use this data sample to perform a singular value decomposition (SVD) analysis of the noise weighted radiance covariance matrix, after mean centering of the data. We then presort the derived eigenvectors based on their associated eigenvalues, $\lambda$'s, from the highest to the lowest eigenvalue. The first five eigenvalues alone were found to account for more than 99% of the total variance contained in the full ensemble (not shown). We only focus our analysis then on the first five eigenfunctions of this analysis, $U_{n,k}$, as a function of frequency $\nu(n)$, where $n$ is the frequency index and k is the eigenfunction index (Figure 3 for band1, 4 for band 2 and 5 for band 3).

The scope of this analysis is to analyze the contribution of each of the 399 selected channels to these most representative top eigenfunctions, as a qualitative measure of their effective representativeness of the total variance contained in the radiance sample.

While eigenfunctions are representative of the variation of combined atmospheric species, by comparison with figure 1, we can distinctly see the first

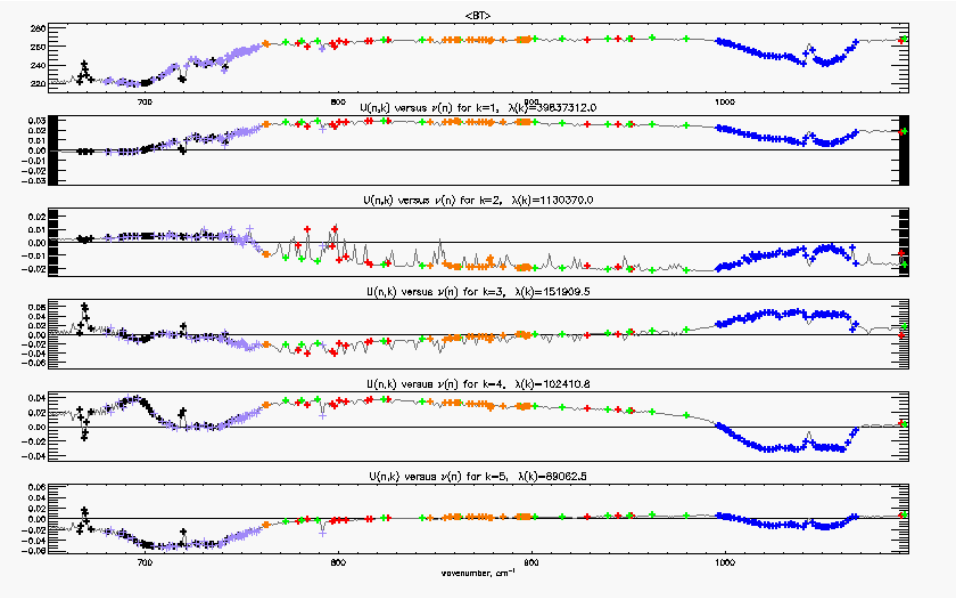


Figure 3: SVD analysis of a global sample of CrIS proxy data. The first 5 eigenfunction are seen to account for more than 99% of the total variance in the sample. Cross symbols indicated the location of the selected channels, color coded according to their main atmospheric sensitivity as in figure 1. In this figure only band 1 is depicted. Top: average brightness temperature.

eigenfunction being mainly representative of the surface temperature signal. We notice that the 24 selected surface temperature and emissivity channels are among the most important contributors to this first eigenvector (green cross symbols).

The highest components of the second eigenvector are found in the 1200-1500 $cm^{-1}$ region where methane, water vapor, $N_2O$ and $SO_2$ are normally active. We have indeed selected the majority of our methane (magenta crosses), water vapor (red crosses), $N_2O$ (yellow crosses) and $SO_2$ (dark purple crosses) sounding channels among the highest peaking channels of this region. The highest components of third and fourth eigenvector fall in the 1000 - 1100 $cm^{-1}$ range which is dominated by the ozone signal. We can confirm that our 53 ozone sounding channels (blue crosses) correspond to the highest peaking channels of both eigenvectors. Eigenvectors 4 and 5 are dominated by the carbon dioxide band signal. The selected temperature and carbon dioxide channels (black and light purple crosses) are among the highest components of these two eigenvectors. The selected carbon monoxide (cyan crosses) and $N_2O$ channels (yellow crosses) are among the highest peaking channels of the first and third eigenvectors.

The analysis just shown indicates a high representativeness of the proposed

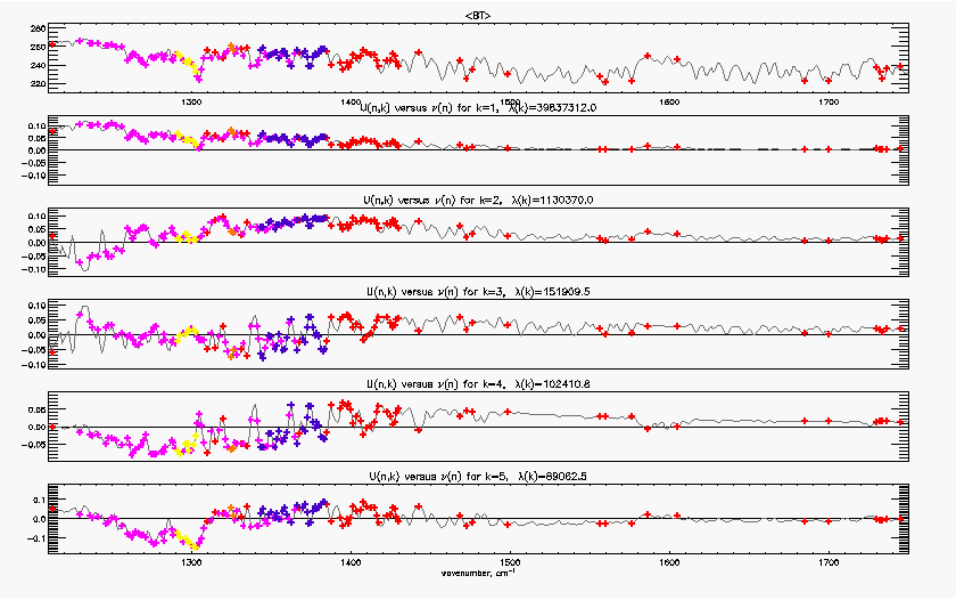


Figure 4: Same as for figure 3, but for band 2.

channel selection in the linear combinations of the orthonormal basis used to describe the main directions of variability contained in the full radiance spectra.

## 3.2 Variance Explained

As anticipated in the introduction, the scope of this channel selection is to optimize the system computational efficiency by selecting channels carrying unique pieces of information such that the internal variability contained in the original spectrum is still fully represented by the selection, up to instrumental noise. We now address the issue of quantitatively computing the actual fraction of the full spectrum variance explained by the proposed channel selection.

We use a CrIS proxy mid-latitude granule sample of full radiance spectra (1305 channels) and compute a polynomial linear fit to the correspondent channel selection spectra, as described by:

$$\Delta R_{N_f,N_s} = A_{N_f,N_{sub}} \Delta R_{N_{sub},N_s} \tag{9}$$

where $N_f$ is the size of the full spectrum (1305 channels), $N_s$ is the number of spectra contained in one granule (5940), $N_sub$ is the size of the channel selection, $\Delta R_{N_f,N_s}$ is the independent variable matrix of mean centered radiance values, $\Delta R_{N_{sub},N_s}$ is the corresponding predictor matrix and $A_{N_f,N_{sub}}$ is the regression coefficient matrix, given by:

$$A_{N_f,N_{sub}} = \Delta R_{N_f,N_s} \Delta R^T_{N_s,N_{sub}} [\Delta R_{N_{sub},N_s} \Delta R^T_{N_s,N_{sub}}]^{-1} \tag{10}$$

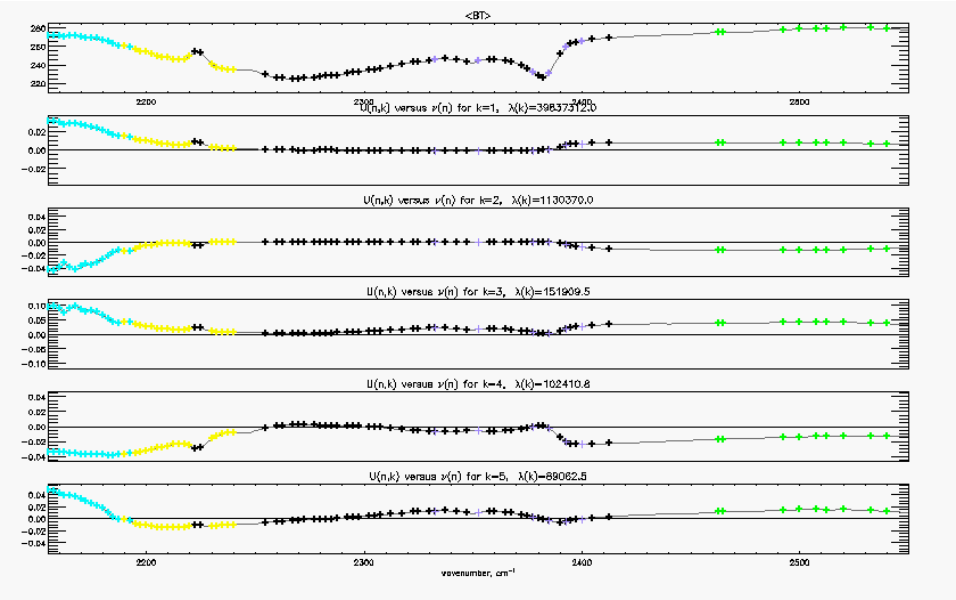


Figure 5: Same as for figure 3, but for band 3.

Once $A_{N_f,N_{sub}}$ is computed, we can derive the calculated $N_f x N_s$ matrix, as in:

$$\Delta R^{calc}_{N_f,N_s} = A_{N_f,N_{sub}} \Delta R_{N_{sub},N_s} \tag{11}$$

We then compare the variance contained in the original spectra, $Var_{tot}$ with the residual sum of squares, $Var_{err}$. Specifically, from the ratio of these two terms we derive what in some texts is referred to as the *coefficient of determination*, $D$, [5], defined as:

$$D = 1 - Var^{err}/Var^{tot} \tag{12}$$

In statistical methods, $D$ is a metric used to determine the goodness of a fit to a model. In regression, $D$ is a statistical measure of how close is the fit to the original data points. The closer $D$ to unity, the better is the fit, that is to say the closer are the predictors (in our case, the actual selected channels) to explain the total variance of the original data sample.

The coefficient of determination is a useful tool for testing the impact of new channels that are either used as a replacement of old ones or that have been incrementally added to a pre-existing selection. Test channels are kept in the selection if they contribute at increasing the total variance explained. In least squares regressions though, like in our case, $D$ increases with the number of predictors. As such, $D$ is not meaningful for comparing selections differing by the actual number of channels. For a meaningful comparison then, we resort to an *adjusted* coefficient of determination, $D^{adj}$, defined as:

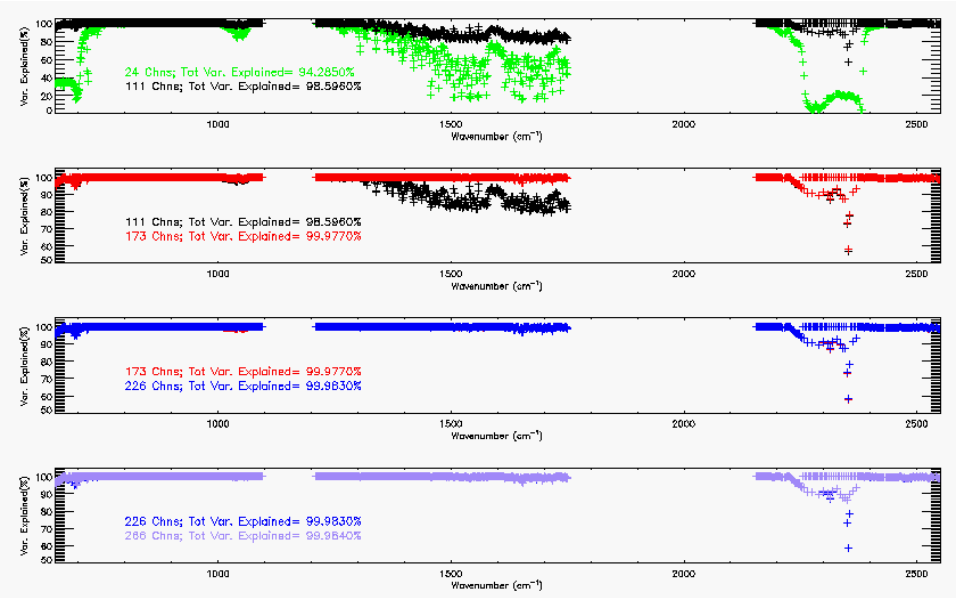


Figure 6: Percentage variance explained. Different colors indicate different channel subset used as predictors. Green curve: surface temperature channel selection only (24 channels). Black curve: previous subset plus 87 temperature sensitive channels. Red curve: like black curve, with 62 additional water vapor sounding channels. Blue: 53 additional ozone sounding channels. Light purple: 53 additional carbon dioxide sounding channels. Captions on figure report the total variance explained by the channel subset. See text for explanation.

$$D^{adj} = 1 - (Var^{err}/Var^{tot})(dof_{tot}/dof_{err}) \tag{13}$$

which represents a statistically unbiased version of $D$. Here $dof_{tot}$ is the degree of freedom of the population variance of the dependent variable and is given by ${N_s}^{tot} - 1$, where ${N_s}^{tot}$ is the sample size of the dependent variable population. $df_{err}$ is the degree of freedom of the predictor population variance, ${N_s}^{tot} - N_{sub} - 1$, where $N_{sub}$ is again the number of predictors (selected channels).

We first compute the coefficient of determination for each channel. The variance contained in the original sample, $Var^{tot}(n)$ and the residual sum of squares, $Var^{err}(n)$ corresponding to channel $\nu$ of index n, are defined by equation 14 and equation 15, respectively:

$$Var^{tot}(n) = \sum_{s=1}^{N_s}[\Delta R_s(n) - (1/N_s)(\sum_{s=1}^{N_s}\Delta R_s(n))]^2 \tag{14}$$

$$Var^{err}(n) = \sum_{s=1}^{N_s}[\Delta R_s(n) - {\Delta R_s}^{calc}(n)]^2 \tag{15}$$

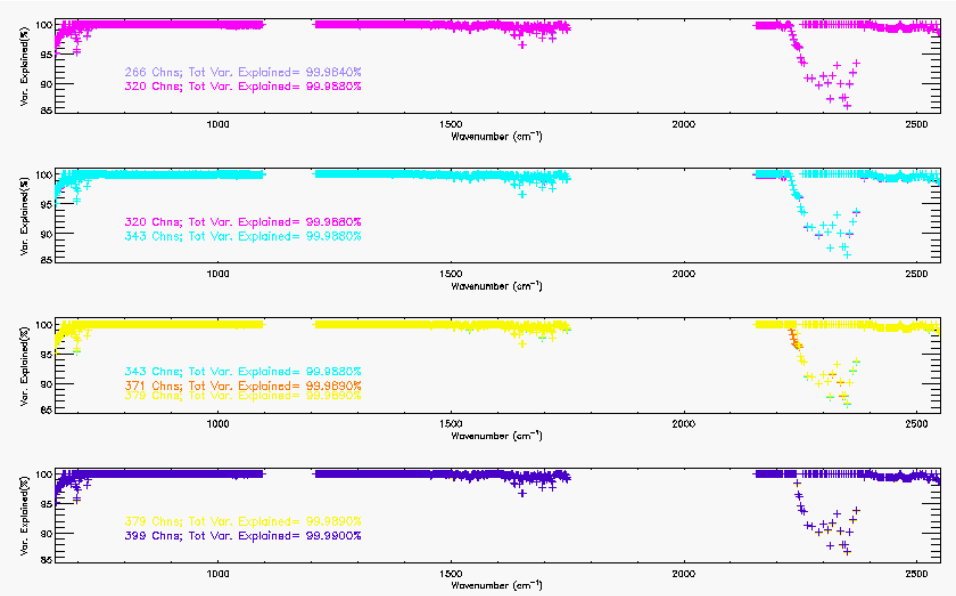


Figure 7: Same as Figure 6. The magenta curve is due to the addition of 54 methane sounding channels. The cyan curve represents the impact of 27 additional carbon monoxide sounding channels. The orange curve refers to the addition of 28 $HNO_3$ sounding channels, the yellow to 24 $N_2O$ and the dark purple to 24 $SO_2$ additional sounding channels. For comparison, the results of a channel subset addition are plotted on top of the results of the previous partial selection. Captions on figure report the total population variance explained by the channel subset. See text for explanation.

We then have, for each channel:

$$D^{adj}(n) = 1 - [Var^{err}(n)/Var^{tot}(n)][(N_s - 1)/(N_s - N_{sub} - 1)] \qquad (16)$$

For completeness, we have plotted the full sequence of improvements obtained by incrementally adding each of the ten channel subsets described in the previous sessions, each including channels mainly sensitive to a given atmospheric species of interest. Results are plotted in figure 6 and 7. For comparison, the results of a channel subset addition are plotted on top of the results of the previous partial selection. We use the same color code of previous figures.

We start by considering the sole 24 selected surface temperature sensitive channels, and we perform the regression as in equations 9, 10 and 11. We then compute the coefficient of determination for the full spectrum, according to equations 14, 15 and 16. Here $N_{sub}$=24. Green symbols on figure 6 indicate the percentage variance explained by the selected 24 surface temperature and emissivity channels. Regions of the spectrum from where these 24 channels

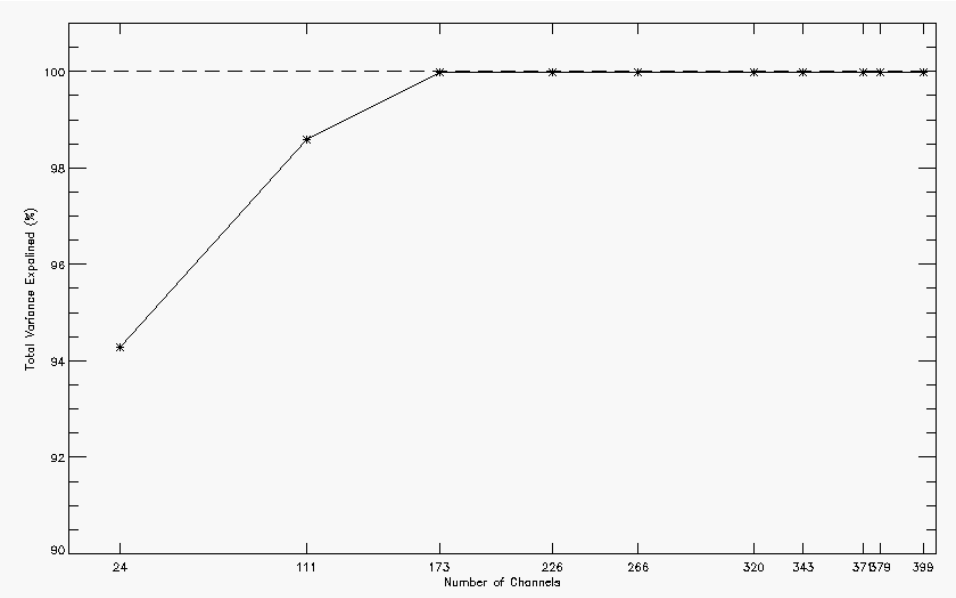


Figure 8: Total population variance explained by each channel subset.

were selected are almost completely explained. This was expected due to the redundancy present across the spectrum.

When we add the 87 temperature channels ($670cm^{-1}$ and $2300cm^{-1}$ region) we considerably improve the variance explained across most of the longwave and shortwave regions. The addition of the 62 selected water vapor channels (which mainly fall in the 1200 - 1700 $cm^{-1}$ region) brings the explained variance in the full mid wave band to more than 99% (red cross symbols). A few percentage more is gained in the 1000 - 1100 $cm^{-1}$ region with the addition of the 53 ozone sounding channels (blue cross symbols) and a few percentage improvement is obtained with the addition of the selected 53 $CO_2$ channels in the shortwave region. The addition of the remaining trace gas subsets brings an improvement of the order of $10^{-3}$ across the spectrum, as shown in figure 7. The reader should notice the change of scale in the reported values of the y axis. The magenta curve is due to the addition of 54 methane sounding channels. The cyan curve represents the impact of 27 additional carbon monoxide sounding channels. The orange curve refers to the addition of 28 $HNO_3$ sounding channels, the yellow to 24 $N_2O$ and the dark purple to 24 $SO_2$ additional sounding channels.

In conclusion, the full 399 channel selection is seen to account for more than 99% of the total variance across the whole spectrum, except for the 600 - 700 $cm^{-1}$ and the $1700cm^{-1}$ regions, where the variance explained is about 95% and for the $2200 - 2300cm^{-1}$ region, where it oscillates between 85% and 99%. This result was expected and originates from the lower representativeness of these spectral bands in our channel selection. This choice rested in the high instru-

mental noise of the 600 - 700 $cm^{-1}$ region, in the lower spectral purity of the $1700cm^{-1}$ with respect to the $1400cm^{-1}$ band (from where we have preferentially selected most of the water vapor channels), and in the high instrumental and calibration noise of the shortwave band. For the reasons just explained, retrieval users generally tend to avoid these low signal to noise spectral regions. Accordingly, we do not expect the lower representativeness of these regions to be penalizing in terms of retrieval application performance.

We now summarize the previous discussion by investigating the variance of the full population in the sample. We define:

$$VAR^{TOT} = \sum_{n=1}^{N_f} Var^{tot}(n) \tag{17}$$

$$VAR^{ERR} = \sum_{n=1}^{N_f} Var^{tot}(n) \tag{18}$$

We then have, for the total population variance explained by each subset:

$$D^{adj\,TOT} = 1 - [VAR^{ERR}/VAR^{TOT}][(N_f * N_s - 1)/(N_f * N_s - N_{sub} - 1)] \tag{19}$$

Results for the total variance explained, $D^{adj\,TOT}$, upon the incremental addition of each subset are listed as captions on figure 6 and 7 and are summarized in figure 8. From this analysis we can see that the first 173 channels including surface and profile temperature and water vapor sensitive channels, are able to already account for more than 99% of the total variability contained in the full sample, while the total variance explained by the complete 399 channel selection is equal to about 99.99%. The case under exam is a mid-latitude case, but tests have been conducted globally and showed equivalent results.

The results just shown confirm that the internal variability contained in the original spectrum is fully explained by the proposed channel selection up to instrumental noise, implying that no significant penalty will be paid in terms of information performance and retrieval application.

# 4 Conclusions and Future Work

We have described the NOAA/NESDIS physically-based methodology for the near real time channel selection of the Cross-track Infrared Sounder. This channel selection is composed of 24 surface temperature and emissivity sounding channels, 87 temperature sounding channels, 62 water vapor, 53 ozone, 27 carbon monoxide, 54 methane, 53 carbon dioxide, 24 $N_2O$, 28 $HNO_3$ and 24 $SO_2$ sounding channels. The described methodology takes in great care spectral purity and vertical sensitivity features, as well as instrumental and apodization noise properties of the channels. A detailed PCA analysis was performed to

identify the information content carried by this selection. The proposed channel selection is found to carry a high representativeness of the atmospheric variability contained in the full radiance spectra. Furthermore, from a regression analysis, we found that the total internal variability contained in the original spectrum is fully explained by the proposed channel selection up to instrumental noise, implying that no significant penalty will be paid in terms of information content and retrieval performance.

Test applications have shown this channel selection to be significantly advantageous in terms of computational efficiency. For example, the computational time of routine operations, such as the computation of radiance covariance matrices, have been observed to improve by a factor of 10 when going from assimilating full spectra down to the 399 channel selection.

The methodology described in this paper has been previously adopted for the operational channel selection of the AIRS and IASI sensors, [15], [7]. National Weather Prediction users have also found great advantage in employing these AIRS and IASI near real time channel selections to expedite data assimilation processing, while guaranteeing good quality in the retrieval results [8].

Existing methodologies, as described in [12], [11] and [3], follow Rodgers statistical iterative methodology [13] where successive tests are performed on the incremental addition of each channels. At each addition, the channel is retained if the information content (based on the entropy of the system) is observed to increase. For near real time operational applications, a *constant* channel selection is normally used, which is derived as an average from multiple optimal selections computed over the globe.

Differently from Rodgers's statistical technique [13], the NOAA/NESDIS methodology described in this paper employs a physically-based procedure where channels are selected solely upon their spectral properties: high priority is given to spectral purity, avoidance of redundancy and vertical sensitivity properties, along with low instrumental noise and global optimality.

Fourrie and Thepaut (2002) have tested the global optimality of the ECMWF *constant* channel selection and compared it to the AIRS NOAA/NESDIS channel selection. They found the performance of the two selections to be comparable, with the NOAA/NESDIS selection providing global optimality with respect to different background error specifications.

We can expect the proposed near real time CrIS channel selection to carry on AIRS and IASI heritage with similar robustness and global optimality. A cross-comparison of the information content contained in the AIRS, IASI and CrIS operational channel selections is under exam. Vertical resolution and degree of freedom of the signal will be also part of a separate study, once the CrIS NOAA/NESDIS retrieval algorithm is fully optimized and retrieval products become operationally available.

# 5 Appendix 1

**T.1: The NOAA/NESDIS CrIS Channel Selection (See legend at the bottom)**

| I | $cm^{-1}$ | Chn Sensitivity | $\tau_{fix}$ | $\tau_{HO_2}$ | $\tau_{O_3}$ |
|---|---|---|---|---|---|
| 27 | 666.250 | T, CF, CH | 0.00 | 0.68 | 0.98 |
| 28 | 666.875 | T, CF, CH | 0.00 | 0.68 | 0.89 |
| 31 | 668.750 | T, CF, CH | 0.00 | 0.69 | 1.00 |
| 32 | 669.375 | T, CF, CH | 0.00 | 0.69 | 0.90 |
| 33 | 670.000 | T, CF, CH | 0.00 | 0.69 | 0.99 |
| 37 | 672.500 | T, CF, CH | 0.00 | 0.70 | 0.97 |
| 49 | 680.000 | $CO_2$ | 0.00 | 0.71 | 0.97 |
| 51 | 681.250 | T, CF, CH | 0.00 | 0.71 | 0.98 |
| 53 | 682.500 | $CO_2$ | 0.00 | 0.72 | 0.97 |
| 59 | 686.250 | $CO_2$ | 0.00 | 0.72 | 0.95 |
| 61 | 687.500 | T, CF, CH | 0.00 | 0.71 | 0.94 |
| 63 | 688.750 | T, CF, CH, $CO_2$ | 0.00 | 0.73 | 0.96 |
| 64 | 689.375 | T, CF, CH | 0.00 | 0.73 | 0.87 |
| 65 | 690.000 | T, CF, CH | 0.00 | 0.73 | 0.95 |
| 67 | 691.250 | $CO_2$ | 0.00 | 0.73 | 0.93 |
| 69 | 692.500 | T, CF, CH | 0.00 | 0.74 | 0.88 |
| 71 | 693.750 | $CO_2$ | 0.00 | 0.73 | 0.97 |
| 73 | 695.000 | T, CF, CH | 0.00 | 0.74 | 0.97 |
| 75 | 696.250 | T, CF, CH, $CO_2$ | 0.00 | 0.74 | 0.95 |
| 79 | 698.750 | T, CF, CH | 0.00 | 0.75 | 0.97 |
| 80 | 699.375 | T, CF, CH | 0.00 | 0.25 | 0.85 |
| 81 | 700.000 | T, CF, CH | 0.00 | 0.75 | 0.97 |
| 83 | 701.250 | T, CF, CH | 0.00 | 0.75 | 0.98 |
| 85 | 702.500 | T, CF, CH | 0.00 | 0.75 | 0.99 |
| 87 | 703.750 | T, CF, CH | 0.00 | 0.70 | 0.98 |
| 88 | 704.375 | T, CF, CH | 0.00 | 0.05 | 0.80 |
| 89 | 705.000 | $CO_2$ | 0.00 | 0.62 | 0.95 |
| 93 | 707.500 | T, CF, CH | 0.00 | 0.68 | 0.95 |
| 95 | 708.750 | $CO_2$ | 0.00 | 0.76 | 0.89 |
| 96 | 709.375 | T, CF, CH | 0.00 | 0.40 | 0.88 |
| 99 | 711.250 | $CO_2$ | 0.00 | 0.76 | 0.96 |
| 101 | 712.500 | $CO_2$ | 0.01 | 0.75 | 0.93 |
| 102 | 713.125 | T, CF, CH, $CO_2$ | 0.01 | 0.49 | 0.92 |
| 104 | 714.375 | $CO_2$ | 0.02 | 0.50 | 0.92 |
| 106 | 715.625 | T, CF, CH | 0.04 | 0.74 | 0.91 |
| 107 | 716.250 | $CO_2$ | 0.03 | 0.76 | 0.92 |
| 111 | 718.750 | T, CF, CH | 0.00 | 0.78 | 0.93 |
| 113 | 720.000 | T, CF, CH | 0.00 | 0.78 | 0.95 |
| 116 | 721.875 | T, CF, CH, $CO_2$ | 0.04 | 0.74 | 0.93 |
| 120 | 724.375 | $CO_2$ | 0.14 | 0.77 | 0.96 |
| 123 | 726.250 | T, CF, CH, $CO_2$ | 0.14 | 0.78 | 0.97 |

**T1: The NOAA/NESDIS CrIS Channel Selection (See legend at the bottom)**

| I | $cm^{-1}$ | Chn Sensitivity | $\tau_{fix}$ | $\tau_{HO_2}$ | $\tau_{O_3}$ |
|---|---|---|---|---|---|
| 124 | 726.875 | T, CF, CH | 0.09 | 0.77 | 0.97 |
| 125 | 727.500 | T, CF, CH | 0.11 | 0.76 | 0.97 |
| 126 | 728.125 | $CO_2$ | 0.10 | 0.72 | 0.96 |
| 130 | 730.625 | $CO_2$ | 0.01 | 0.08 | 0.96 |
| 132 | 731.875 | T, CF, CH | 0.05 | 0.59 | 0.98 |
| 133 | 732.500 | $CO_2$ | 0.09 | 0.75 | 0.97 |
| 136 | 734.375 | T, CF, CH | 0.09 | 0.78 | 0.97 |
| 137 | 735.000 | $CO_2$ | 0.08 | 0.80 | 0.96 |
| 138 | 735.625 | T, CF, CH | 0.10 | 0.79 | 0.97 |
| 142 | 738.125 | T, CF, CH | 0.09 | 0.78 | 0.97 |
| 143 | 738.750 | $CO_2$ | 0.10 | 0.79 | 0.98 |
| 144 | 739.375 | $CO_2$ | 0.07 | 0.68 | 0.98 |
| 145 | 740.000 | $CO_2$ | 0.06 | 0.53 | 0.98 |
| 147 | 741.250 | $CO_2$ | 0.01 | 0.65 | 0.97 |
| 148 | 741.875 | T, CF, CH | 0.02 | 0.53 | 0.96 |
| 150 | 743.125 | T, CF, CH, $CO_2$ | 0.18 | 0.64 | 0.94 |
| 151 | 743.750 | $CO_2$ | 0.11 | 0.47 | 0.96 |
| 153 | 745.000 | $CO_2$ | 0.06 | 0.22 | 0.97 |
| 154 | 745.625 | T, CF, CH, $CO_2$ | 0.20 | 0.65 | 0.98 |
| 155 | 746.250 | $CO_2$ | 0.28 | 0.77 | 0.98 |
| 157 | 747.500 | $CO_2$ | 0.29 | 0.70 | 0.98 |
| 158 | 748.125 | $CO_2$ | 0.21 | 0.61 | 0.98 |
| 159 | 748.750 | T, CF, CH, $CO_2$ | 0.25 | 0.64 | 0.98 |
| 160 | 749.375 | $CO_2$ | 0.30 | 0.72 | 0.98 |
| 161 | 750.000 | $CO_2$ | 0.29 | 0.78 | 0.96 |
| 162 | 750.625 | $CO_2$ | 0.37 | 0.79 | 0.95 |
| 163 | 751.250 | $CO_2$ | 0.29 | 0.74 | 0.96 |
| 164 | 751.875 | $CO_2$ | 0.27 | 0.55 | 0.98 |
| 165 | 752.500 | $CO_2$ | 0.24 | 0.50 | 0.98 |
| 166 | 753.125 | $CO_2$ | 0.27 | 0.58 | 0.98 |
| 168 | 754.375 | $CO_2$ | 0.13 | 0.27 | 0.98 |
| 170 | 755.625 | $CO_2$ | 0.34 | 0.62 | 0.98 |
| 171 | 756.250 | $CO_2$ | 0.41 | 0.72 | 0.98 |
| 173 | 757.500 | $CO_2$ | 0.45 | 0.81 | 0.97 |
| 175 | 758.750 | $CO_2$ | 0.54 | 0.82 | 0.98 |
| 181 | 762.500 | $HNO_3$ | 0.68 | 0.83 | 0.99 |
| 183 | 763.750 | $HNO_3$ | 0.68 | 0.83 | 0.98 |
| 198 | 773.125 | Srf | 0.77 | 0.83 | 0.99 |
| 208 | 779.375 | $H_2O$ | 0.55 | 0.58 | 0.99 |
| 211 | 781.250 | Srf | 0.80 | 0.83 | 0.99 |
| 216 | 784.375 | $H_2O$ | 0.30 | 0.31 | 0.99 |
| 224 | 789.375 | Srf | 0.83 | 0.85 | 1.00 |
| 228 | 791.875 | $CO_2$ | 0.42 | 0.81 | 1.00 |

**T1: The NOAA/NESDIS CrIS Channel Selection (See legend at the bottom)**

| I | $cm^{-1}$ | Chn Sensitivity | $\tau_{fix}$ | $\tau_{HO_2}$ | $\tau_{O_3}$ |
|---|---|---|---|---|---|
| 236 | 796.875 | $H_2O$ | 0.55 | 0.57 | 1.00 |
| 238 | 798.125 | $H_2O$ | 0.29 | 0.31 | 1.00 |
| 242 | 800.625 | $H_2O$ | 0.80 | 0.82 | 1.00 |
| 248 | 804.375 | $H_2O$ | 0.73 | 0.76 | 1.00 |
| 266 | 815.625 | $H_2O$ | 0.82 | 0.84 | 1.00 |
| 268 | 816.875 | $H_2O$ | 0.85 | 0.87 | 1.00 |
| 279 | 823.750 | Srf | 0.87 | 0.88 | 1.00 |
| 283 | 826.250 | $H_2O$ | 0.85 | 0.85 | 1.00 |
| 311 | 843.750 | Srf | 0.87 | 0.89 | 1.00 |
| 317 | 847.500 | $HNO_3$ | 0.87 | 0.89 | 1.00 |
| 330 | 855.625 | $HNO_3$ | 0.85 | 0.85 | 1.00 |
| 333 | 857.500 | $HNO_3$ | 0.89 | 0.89 | 1.00 |
| 334 | 858.125 | $HNO_3$ | 0.87 | 0.88 | 1.00 |
| 338 | 860.625 | $HNO_3$ | 0.89 | 0.90 | 1.00 |
| 340 | 861.875 | $HNO_3$ | 0.90 | 0.90 | 1.00 |
| 341 | 862.500 | $HNO_3$ | 0.89 | 0.90 | 1.00 |
| 342 | 863.125 | Srf | 0.90 | 0.90 | 1.00 |
| 349 | 867.500 | $HNO_3$ | 0.90 | 0.90 | 1.00 |
| 352 | 869.375 | $HNO_3$ | 0.90 | 0.90 | 1.00 |
| 358 | 873.125 | $HNO_3$ | 0.90 | 0.90 | 1.00 |
| 361 | 875.000 | $HNO_3$ | 0.90 | 0.91 | 1.00 |
| 364 | 876.875 | $HNO_3$ | 0.90 | 0.90 | 1.00 |
| 366 | 878.125 | $HNO_3$ | 0.77 | 0.78 | 1.00 |
| 367 | 878.750 | $HNO_3$ | 0.74 | 0.75 | 1.00 |
| 368 | 879.375 | $HNO_3$ | 0.85 | 0.87 | 1.00 |
| 378 | 885.625 | $HNO_3$ | 0.89 | 0.90 | 1.00 |
| 390 | 893.125 | $HNO_3$ | 0.91 | 0.92 | 1.00 |
| 391 | 893.750 | $HNO_3$ | 0.91 | 0.91 | 1.00 |
| 392 | 894.375 | Srf | 0.91 | 0.92 | 1.00 |
| 394 | 895.625 | $HNO_3$ | 0.90 | 0.91 | 1.00 |
| 395 | 896.250 | $HNO_3$ | 0.90 | 0.91 | 1.00 |
| 396 | 896.875 | $HNO_3$ | 0.90 | 0.91 | 1.00 |
| 397 | 897.500 | $HNO_3$ | 0.89 | 0.89 | 1.00 |
| 398 | 898.125 | $HNO_3$ | 0.89 | 0.90 | 1.00 |
| 399 | 898.750 | $HNO_3$ | 0.91 | 0.91 | 1.00 |
| 404 | 901.875 | Srf | 0.91 | 0.92 | 1.00 |
| 427 | 916.250 | Srf | 0.90 | 0.92 | 1.00 |
| 447 | 928.750 | $H_2O$ | 0.87 | 0.91 | 1.00 |
| 464 | 939.375 | Srf | 0.91 | 0.93 | 1.00 |
| 473 | 945.000 | $H_2O$ | 0.88 | 0.90 | 1.00 |
| 482 | 950.625 | Srf | 0.91 | 0.94 | 1.00 |
| 484 | 951.875 | $H_2O$ | 0.91 | 0.94 | 1.00 |
| 501 | 962.500 | Srf | 0.93 | 0.94 | 1.00 |

**T1: The NOAA/NESDIS CrIS Channel Selection (See legend at the bottom)**

| I | $cm^{-1}$ | Chn Sensitivity | $\tau_{fix}$ | $\tau_{HO_2}$ | $\tau_{O_3}$ |
|---|---|---|---|---|---|
| 529 | 980.000 | Srf | 0.90 | 0.94 | 0.99 |
| 556 | 996.875 | $O_3$ | 0.85 | 0.95 | 0.89 |
| 557 | 997.500 | $O_3$ | 0.83 | 0.95 | 0.88 |
| 558 | 998.125 | $O_3$ | 0.81 | 0.93 | 0.87 |
| 560 | 999.375 | $O_3$ | 0.78 | 0.92 | 0.85 |
| 561 | 1000.000 | $O_3$ | 0.77 | 0.91 | 0.84 |
| 562 | 1000.625 | $O_3$ | 0.77 | 0.91 | 0.84 |
| 564 | 1001.875 | $O_3$ | 0.78 | 0.95 | 0.82 |
| 565 | 1002.500 | $O_3$ | 0.76 | 0.95 | 0.81 |
| 566 | 1003.125 | $O_3$ | 0.75 | 0.93 | 0.80 |
| 569 | 1005.000 | $O_3$ | 0.71 | 0.94 | 0.76 |
| 573 | 1007.500 | $O_3$ | 0.67 | 0.95 | 0.71 |
| 574 | 1008.125 | $O_3$ | 0.68 | 0.95 | 0.72 |
| 577 | 1010.000 | $O_3$ | 0.55 | 0.83 | 0.66 |
| 580 | 1011.875 | $O_3$ | 0.58 | 0.94 | 0.62 |
| 581 | 1012.500 | $O_3$ | 0.58 | 0.95 | 0.62 |
| 584 | 1014.375 | $O_3$ | 0.45 | 0.79 | 0.57 |
| 585 | 1015.000 | $O_3$ | 0.50 | 0.85 | 0.59 |
| 587 | 1016.250 | $O_3$ | 0.52 | 0.95 | 0.55 |
| 590 | 1018.125 | $O_3$ | 0.43 | 0.86 | 0.51 |
| 591 | 1018.750 | $O_3$ | 0.45 | 0.93 | 0.49 |
| 594 | 1020.625 | $O_3$ | 0.43 | 0.95 | 0.45 |
| 597 | 1022.500 | $O_3$ | 0.43 | 0.95 | 0.45 |
| 598 | 1023.125 | $O_3$ | 0.42 | 0.96 | 0.44 |
| 601 | 1025.000 | $O_3$ | 0.40 | 0.96 | 0.42 |
| 604 | 1026.875 | $O_3$ | 0.40 | 0.95 | 0.42 |
| 607 | 1028.750 | $O_3$ | 0.33 | 0.79 | 0.43 |
| 611 | 1031.250 | $O_3$ | 0.39 | 0.93 | 0.43 |
| 614 | 1033.125 | $O_3$ | 0.38 | 0.94 | 0.41 |
| 616 | 1034.375 | $O_3$ | 0.38 | 0.96 | 0.40 |
| 617 | 1035.000 | $O_3$ | 0.34 | 0.95 | 0.36 |
| 619 | 1036.250 | $O_3$ | 0.34 | 0.96 | 0.36 |
| 622 | 1038.125 | $O_3$ | 0.28 | 0.94 | 0.30 |
| 626 | 1040.625 | $O_3$ | 0.21 | 0.96 | 0.22 |
| 628 | 1041.875 | $O_3$ | 0.46 | 0.93 | 0.51 |
| 634 | 1045.625 | $O_3$ | 0.55 | 0.96 | 0.60 |
| 637 | 1047.500 | $O_3$ | 0.33 | 0.96 | 0.36 |
| 638 | 1048.125 | $O_3$ | 0.30 | 0.96 | 0.32 |
| 640 | 1049.375 | $O_3$ | 0.27 | 0.87 | 0.32 |
| 641 | 1050.000 | $O_3$ | 0.26 | 0.92 | 0.31 |
| 642 | 1050.625 | $O_3$ | 0.20 | 0.90 | 0.25 |
| 644 | 1051.875 | $O_3$ | 0.23 | 0.90 | 0.28 |
| 646 | 1053.125 | $O_3$ | 0.22 | 0.96 | 0.24 |

**T1: The NOAA/NESDIS CrIS Channel Selection (See legend at the bottom)**

| I | $cm^{-1}$ | Chn Sensitivity | $\tau_{fix}$ | $\tau_{HO_2}$ | $\tau_{O_3}$ |
|---|---|---|---|---|---|
| 647 | 1053.750 | $O_3$ | 0.22 | 0.96 | 0.24 |
| 650 | 1055.625 | $O_3$ | 0.21 | 0.82 | 0.28 |
| 651 | 1056.250 | $O_3$ | 0.23 | 0.91 | 0.27 |
| 652 | 1056.875 | $O_3$ | 0.28 | 0.96 | 0.31 |
| 654 | 1058.125 | $O_3$ | 0.32 | 0.94 | 0.35 |
| 655 | 1058.750 | $O_3$ | 0.31 | 0.93 | 0.35 |
| 657 | 1060.000 | $O_3$ | 0.30 | 0.87 | 0.35 |
| 659 | 1061.250 | $O_3$ | 0.38 | 0.95 | 0.41 |
| 663 | 1063.750 | $O_3$ | 0.56 | 0.95 | 0.59 |
| 667 | 1066.250 | $O_3$ | 0.43 | 0.58 | 0.78 |
| 670 | 1068.125 | $O_3$ | 0.80 | 0.96 | 0.87 |
| 707 | 1091.250 | $H_2O$ | 0.65 | 0.69 | 0.98 |
| 710 | 1093.125 | Srf | 0.91 | 0.96 | 0.97 |
| 713 | 1095.000 | Srf | 0.91 | 0.96 | 0.97 |
| 716 | 1212.500 | $H_2O$ | 0.29 | 0.30 | 1.00 |
| 730 | 1230.000 | $CH_4$ | 0.71 | 0.88 | 1.00 |
| 735 | 1236.250 | $CH_4$ | 0.59 | 0.79 | 1.00 |
| 736 | 1237.500 | $CH_4$ | 0.54 | 0.74 | 1.00 |
| 739 | 1241.250 | $CH_4$ | 0.55 | 0.71 | 1.00 |
| 743 | 1246.250 | $CH_4$ | 0.45 | 0.71 | 1.00 |
| 744 | 1247.500 | $CH_4$ | 0.50 | 0.77 | 1.00 |
| 746 | 1250.000 | $CH_4$ | 0.53 | 0.73 | 1.00 |
| 748 | 1252.500 | $CH_4$ | 0.40 | 0.58 | 1.00 |
| 751 | 1256.250 | $CH_4$ | 0.41 | 0.67 | 1.00 |
| 754 | 1260.000 | $CH_4$ | 0.03 | 0.08 | 1.00 |
| 755 | 1261.250 | $CH_4$ | 0.07 | 0.20 | 1.00 |
| 756 | 1262.500 | $CH_4$ | 0.16 | 0.43 | 1.00 |
| 757 | 1263.750 | $CH_4$ | 0.18 | 0.42 | 1.00 |
| 758 | 1265.000 | $CH_4$ | 0.11 | 0.25 | 1.00 |
| 760 | 1267.500 | $CH_4$ | 0.05 | 0.14 | 1.00 |
| 761 | 1268.750 | $CH_4$ | 0.01 | 0.05 | 1.00 |
| 762 | 1270.000 | $CH_4$ | 0.00 | 0.01 | 1.00 |
| 763 | 1271.250 | $CH_4$ | 0.00 | 0.01 | 1.00 |
| 766 | 1275.000 | $CH_4$ | 0.19 | 0.59 | 1.00 |
| 767 | 1276.250 | $CH_4$ | 0.19 | 0.71 | 1.00 |
| 768 | 1277.500 | $CH_4$ | 0.23 | 0.74 | 1.00 |
| 771 | 1281.250 | $CH_4$ | 0.13 | 0.31 | 1.00 |
| 772 | 1282.500 | $CH_4$ | 0.13 | 0.43 | 1.00 |
| 773 | 1283.750 | $CH_4$ | 0.11 | 0.26 | 1.00 |
| 776 | 1287.500 | $CH_4$ | 0.03 | 0.09 | 1.00 |
| 777 | 1288.750 | $CH_4$ | 0.05 | 0.16 | 1.00 |
| 778 | 1290.000 | $CH_4$ | 0.11 | 0.25 | 1.00 |
| 779 | 1291.250 | $N_2O$ | 0.17 | 0.36 | 1.00 |
| 780 | 1292.500 | $CH_4$, $N_2O$ | 0.17 | 0.47 | 1.00 |

**T1: The NOAA/NESDIS CrIS Channel Selection (See legend at the bottom)**

| I | $cm^{-1}$ | Chn Sensitivity | $\tau_{fix}$ | $\tau_{HO_2}$ | $\tau_{O_3}$ |
|---|---|---|---|---|---|
| 782 | 1295.00 | $CH_4$ | 0.10 | 0.41 | 1.0 |
| 783 | 1296.25 | $CH_4$, $N_2O$ | 0.05 | 0.21 | 1.0 |
| 784 | 1297.50 | $N_2O$ | 0.07 | 0.30 | 1.0 |
| 785 | 1298.75 | $N_2O$ | 0.13 | 0.63 | 1.0 |
| 786 | 1300.00 | $CH_4$ | 0.12 | 0.67 | 1.0 |
| 787 | 1301.25 | $CH_4$, $N_2O$ | 0.07 | 0.70 | 1.0 |
| 788 | 1302.50 | $CH_4$, $N_2O$ | 0.03 | 0.65 | 1.0 |
| 789 | 1303.75 | $CH_4$ | 0.01 | 0.78 | 1.0 |
| 790 | 1305.00 | $CH_4$ | 0.00 | 0.28 | 1.0 |
| 791 | 1306.25 | $CH_4$ | 0.02 | 0.12 | 1.0 |
| 792 | 1307.50 | $CH_4$ | 0.03 | 0.07 | 1.0 |
| 794 | 1310.00 | $H_2O$ | 0.10 | 0.17 | 1.0 |
| 796 | 1312.50 | $CH_4$ | 0.01 | 0.02 | 1.0 |
| 798 | 1315.00 | $H_2O$ | 0.00 | 0.01 | 1.0 |
| 800 | 1317.50 | $CH_4$ | 0.00 | 0.00 | 1.0 |
| 802 | 1320.00 | $H_2O$ | 0.00 | 0.00 | 1.0 |
| 803 | 1321.25 | $CH_4$ | 0.02 | 0.02 | 1.0 |
| 804 | 1322.50 | $CH_4$ | 0.04 | 0.05 | 1.0 |
| 806 | 1325.00 | $HNO_3$ | 0.16 | 0.18 | 1.0 |
| 807 | 1326.25 | $HNO_3$ | 0.13 | 0.20 | 1.0 |
| 808 | 1327.50 | $CH_4$ | 0.08 | 0.15 | 1.0 |
| 809 | 1328.75 | $CH_4$ | 0.10 | 0.13 | 1.0 |
| 811 | 1331.25 | $H_2O$ | 0.15 | 0.22 | 1.0 |
| 812 | 1332.50 | $CH_4$ | 0.08 | 0.18 | 1.0 |
| 814 | 1335.00 | $H_2O$ | 0.04 | 0.04 | 1.0 |
| 816 | 1337.50 | $CH_4$ | 0.00 | 0.00 | 1.0 |
| 819 | 1341.25 | $CH_4$ | 0.00 | 0.00 | 1.0 |
| 820 | 1342.50 | $CH_4$ | 0.01 | 0.03 | 1.0 |
| 821 | 1343.75 | $SO_2$ | 0.03 | 0.05 | 1.0 |
| 822 | 1345.00 | $H_2O$, $SO_2$ | 0.05 | 0.07 | 1.0 |
| 823 | 1346.25 | $CH_4$ | 0.03 | 0.07 | 1.0 |
| 824 | 1347.50 | $CH_4$ | 0.02 | 0.04 | 1.0 |
| 825 | 1348.75 | $SO_2$ | 0.01 | 0.01 | 1.0 |
| 826 | 1350.00 | $SO_2$ | 0.01 | 0.01 | 1.0 |
| 827 | 1351.25 | $CH_4$ | 0.02 | 0.03 | 1.0 |
| 828 | 1352.50 | $SO_2$ | 0.03 | 0.04 | 1.0 |
| 829 | 1353.75 | $SO_2$ | 0.02 | 0.02 | 1.0 |
| 830 | 1355.00 | $SO_2$ | 0.00 | 0.01 | 1.0 |
| 831 | 1356.25 | $CH_4$ | 0.01 | 0.01 | 1.0 |
| 832 | 1357.50 | $H_2O$, $SO_2$ | 0.01 | 0.01 | 1.0 |
| 833 | 1358.75 | $CH_4$, $SO_2$ | 0.00 | 0.00 | 1.0 |

**T1: The NOAA/NESDIS CrIS Channel Selection (See legend at the bottom)**

| I | $cm^{-1}$ | Chn Sensitivity | $\tau_{fix}$ | $\tau_{HO_2}$ | $\tau_{O_3}$ |
|---|---|---|---|---|---|
| 834 | 1360.00 | $SO_2$ | 0.0 | 0.0 | 1.0 |
| 835 | 1361.25 | $CH_4$ | 0.0 | 0.0 | 1.0 |
| 836 | 1362.50 | $SO_2$ | 0.0 | 0.0 | 1.0 |
| 838 | 1365.000 | $CH_4$ | 0.0 | 0.0 | 1.0 |
| 839 | 1366.250 | $SO_2$ | 0.0 | 0.0 | 1.0 |
| 840 | 1367.500 | $H_2O$ | 0.0 | 0.0 | 1.0 |
| 842 | 1370.000 | $SO_2$ | 0.0 | 0.0 | 1.0 |
| 843 | 1371.250 | $SO_2$ | 0.0 | 0.0 | 1.0 |
| 844 | 1372.500 | $SO_2$ | 0.0 | 0.0 | 1.0 |
| 845 | 1373.750 | $SO_2$ | 0.0 | 0.0 | 1.0 |
| 846 | 1375.000 | $SO_2$ | 0.0 | 0.0 | 1.0 |
| 847 | 1376.250 | $SO_2$ | 0.0 | 0.0 | 1.0 |
| 848 | 1377.500 | $SO_2$ | 0.0 | 0.0 | 1.0 |
| 849 | 1378.750 | $SO_2$ | 0.0 | 0.0 | 1.0 |
| 850 | 1380.000 | $SO_2$ | 0.0 | 0.0 | 1.0 |
| 851 | 1381.250 | $H_2O$, $SO_2$ | 0.0 | 0.0 | 1.0 |
| 852 | 1382.500 | $SO_2$ | 0.0 | 0.0 | 1.0 |
| 853 | 1383.750 | $SO_2$ | 0.0 | 0.0 | 1.0 |
| 854 | 1385.000 | $H_2O$ | 0.0 | 0.0 | 1.0 |
| 856 | 1387.500 | $H_2O$ | 0.0 | 0.0 | 1.0 |
| 861 | 1393.750 | $H_2O$ | 0.0 | 0.0 | 1.0 |
| 862 | 1395.000 | $H_2O$ | 0.0 | 0.0 | 1.0 |
| 864 | 1397.500 | $H_2O$ | 0.0 | 0.0 | 1.0 |
| 865 | 1398.750 | $H_2O$ | 0.0 | 0.0 | 1.0 |
| 866 | 1400.000 | $H_2O$ | 0.0 | 0.0 | 1.0 |
| 867 | 1401.250 | $H_2O$ | 0.0 | 0.0 | 1.0 |
| 869 | 1403.750 | $H_2O$ | 0.0 | 0.0 | 1.0 |
| 871 | 1406.250 | $H_2O$ | 0.0 | 0.0 | 1.0 |
| 872 | 1407.500 | $H_2O$ | 0.0 | 0.0 | 1.0 |
| 874 | 1410.000 | $H_2O$ | 0.0 | 0.0 | 1.0 |
| 876 | 1412.500 | $H_2O$ | 0.0 | 0.0 | 1.0 |
| 878 | 1415.000 | $H_2O$ | 0.0 | 0.0 | 1.0 |
| 879 | 1416.250 | $H_2O$ | 0.0 | 0.0 | 1.0 |
| 880 | 1417.500 | $H_2O$ | 0.0 | 0.0 | 1.0 |
| 884 | 1422.500 | $H_2O$ | 0.0 | 0.0 | 1.0 |
| 886 | 1425.000 | $H_2O$ | 0.0 | 0.0 | 1.0 |
| 887 | 1426.250 | $H_2O$ | 0.0 | 0.0 | 1.0 |
| 888 | 1427.500 | $H_2O$ | 0.0 | 0.0 | 1.0 |
| 889 | 1428.750 | $H_2O$ | 0.0 | 0.0 | 1.0 |
| 890 | 1430.000 | $H_2O$ | 0.0 | 0.0 | 1.0 |
| 900 | 1442.500 | $H_2O$ | 0.0 | 0.0 | 1.0 |
| 921 | 1468.750 | $H_2O$ | 0.0 | 0.0 | 1.0 |
| 924 | 1472.500 | $H_2O$ | 0.0 | 0.0 | 1.0 |

**T1: The NOAA/NESDIS CrIS Channel Selection (See legend at the bottom)**

| I | $cm^{-1}$ | Chn Sensitivity | $\tau_{fix}$ | $\tau_{HO_2}$ | $\tau_{O_3}$ |
|---|---|---|---|---|---|
| 927 | 1476.25 | $H_2O$ | 0.00 | 0.00 | 1.00 |
| 945 | 1498.75 | $H_2O$ | 0.00 | 0.00 | 1.00 |
| 991 | 1556.25 | $H_2O$ | 0.00 | 0.00 | 1.00 |
| 994 | 1560.00 | $H_2O$ | 0.00 | 0.00 | 1.00 |
| 1007 | 1576.25 | $H_2O$ | 0.00 | 0.00 | 1.00 |
| 1015 | 1586.25 | $H_2O$ | 0.00 | 0.00 | 1.00 |
| 1030 | 1605.00 | $H_2O$ | 0.00 | 0.00 | 1.00 |
| 1094 | 1685.00 | $H_2O$ | 0.00 | 0.00 | 1.00 |
| 1106 | 1700.00 | $H_2O$ | 0.00 | 0.00 | 1.00 |
| 1130 | 1730.00 | $H_2O$ | 0.00 | 0.00 | 1.00 |
| 1132 | 1732.50 | $H_2O$ | 0.00 | 0.00 | 1.00 |
| 1133 | 1733.75 | $H_2O$ | 0.00 | 0.00 | 1.00 |
| 1135 | 1736.25 | $H_2O$ | 0.00 | 0.00 | 0.98 |
| 1142 | 1745.00 | $H_2O$ | 0.00 | 0.00 | 1.00 |
| 1147 | 2155.00 | $CO$ | 0.73 | 0.85 | 1.00 |
| 1148 | 2157.50 | $CO$ | 0.75 | 0.89 | 1.00 |
| 1149 | 2160.00 | $CO$ | 0.70 | 0.86 | 1.00 |
| 1150 | 2162.50 | $CO$ | 0.64 | 0.79 | 1.00 |
| 1151 | 2165.00 | $CO$ | 0.69 | 0.88 | 1.00 |
| 1152 | 2167.50 | $CO$ | 0.72 | 0.95 | 1.00 |
| 1153 | 2170.00 | $CO$ | 0.66 | 0.90 | 1.00 |
| 1154 | 2172.50 | $CO$ | 0.63 | 0.89 | 1.00 |
| 1155 | 2175.00 | $CO$ | 0.63 | 0.95 | 1.00 |
| 1156 | 2177.50 | $CO$ | 0.60 | 0.96 | 1.00 |
| 1157 | 2180.00 | $CO$ | 0.52 | 0.92 | 1.00 |
| 1158 | 2182.50 | $CO$ | 0.44 | 0.89 | 1.00 |
| 1159 | 2185.00 | $CO$ | 0.36 | 0.86 | 1.00 |
| 1160 | 2187.50 | $CO$ | 0.32 | 0.86 | 1.00 |
| 1161 | 2190.00 | $CO$, $N_2O$ | 0.33 | 0.94 | 1.00 |
| 1162 | 2192.50 | $CO$ | 0.31 | 0.94 | 1.00 |
| 1163 | 2195.00 | $CO$, $N_2O$ | 0.24 | 0.96 | 1.00 |
| 1164 | 2197.50 | $CO$, $N_2O$ | 0.19 | 0.93 | 1.00 |
| 1165 | 2200.00 | T, CF, $CO$, $N_2O$ | 0.17 | 0.90 | 1.00 |
| 1166 | 2202.50 | T, CF, $CO$, $N_2O$ | 0.15 | 0.89 | 1.00 |
| 1167 | 2205.00 | $CO$, $N_2O$ | 0.11 | 0.89 | 1.00 |
| 1168 | 2207.50 | T, CF, $CO$, $N_2O$ | 0.10 | 0.86 | 1.00 |
| 1169 | 2210.00 | $CO$, $N_2O$ | 0.10 | 0.89 | 1.00 |
| 1170 | 2212.50 | $CO$, $N_2O$ | 0.08 | 0.89 | 1.00 |
| 1171 | 2215.00 | $CO$, $N_2O$ | 0.08 | 0.94 | 1.00 |
| 1172 | 2217.50 | $CO$, $N_2O$ | 0.08 | 0.94 | 1.00 |
| 1173 | 2220.00 | T, CF, $CO$, $N_2O$ | 0.12 | 0.96 | 1.00 |
| 1174 | 2222.50 | T, CF | 0.18 | 0.96 | 1.00 |
| 1175 | 2225.00 | T, CF | 0.16 | 0.93 | 1.00 |
| 1177 | 2230.00 | $N_2O$ | 0.03 | 0.94 | 1.00 |

**T1: The NOAA/NESDIS CrIS Channel Selection (See legend at the bottom)**

| I | $cm^{-1}$ | Chn Sensitivity | $\tau_{fix}$ | $\tau_{HO_2}$ | $\tau_{O_3}$ |
|---|---|---|---|---|---|
| 1178 | 2232.5 | $N_2O$ | 0.02 | 0.93 | 1.00 |
| 1179 | 2235.0 | $N_2O$ | 0.01 | 0.98 | 1.00 |
| 1180 | 2237.5 | $N_2O$ | 0.01 | 0.89 | 1.00 |
| 1181 | 2240.0 | $N_2O$ | 0.01 | 0.98 | 1.00 |
| 1187 | 2255.0 | T, CF | 0.00 | 0.97 | 0.95 |
| 1189 | 2260.0 | T, CF | 0.00 | 0.98 | 0.94 |
| 1190 | 2262.5 | T, CF | 0.00 | 0.72 | 1.00 |
| 1192 | 2267.5 | T, CF | 0.00 | 0.84 | 1.00 |
| 1193 | 2270.0 | T, CF | 0.00 | 0.98 | 0.93 |
| 1194 | 2272.5 | T, CF | 0.00 | 0.84 | 1.00 |
| 1196 | 2277.5 | T, CF | 0.00 | 0.85 | 1.00 |
| 1197 | 2280.0 | T, CF | 0.00 | 0.98 | 0.94 |
| 1198 | 2282.5 | T, CF | 0.00 | 0.73 | 1.00 |
| 1199 | 2285.0 | T, CF | 0.00 | 0.98 | 0.95 |
| 1200 | 2287.5 | T, CF | 0.00 | 0.88 | 1.00 |
| 1202 | 2292.5 | T, CF | 0.00 | 0.98 | 1.00 |
| 1203 | 2295.0 | T, CF | 0.00 | 0.98 | 0.92 |
| 1204 | 2297.5 | T, CF | 0.00 | 0.98 | 1.00 |
| 1206 | 2302.5 | T, CF | 0.00 | 0.98 | 1.00 |
| 1207 | 2305.0 | T, CF | 0.00 | 0.98 | 0.91 |
| 1208 | 2307.5 | T, CF | 0.00 | 0.98 | 1.00 |
| 1210 | 2312.5 | T, CF | 0.00 | 0.98 | 1.00 |
| 1212 | 2317.5 | T, CF | 0.00 | 0.99 | 1.00 |
| 1214 | 2322.5 | T, CF | 0.00 | 0.99 | 1.00 |
| 1215 | 2325.0 | T, CF | 0.00 | 0.99 | 0.93 |
| 1217 | 2330.0 | T, CF | 0.00 | 0.99 | 0.94 |
| 1218 | 2332.5 | T, CF, $CO_2$ | 0.00 | 0.99 | 1.00 |
| 1220 | 2337.5 | T, CF | 0.00 | 0.99 | 1.00 |
| 1222 | 2342.5 | T, CF | 0.00 | 0.99 | 1.00 |
| 1224 | 2347.5 | T, CF | 0.00 | 0.99 | 1.00 |
| 1226 | 2352.5 | $CO_2$ | 0.00 | 0.99 | 1.00 |
| 1228 | 2357.5 | T, CF | 0.00 | 0.99 | 1.00 |
| 1229 | 2360.0 | T, CF | 0.00 | 0.99 | 0.98 |
| 1231 | 2365.0 | T, CF | 0.00 | 0.99 | 0.97 |
| 1232 | 2367.5 | T, CF | 0.00 | 0.99 | 1.00 |
| 1234 | 2372.5 | T, CF | 0.00 | 0.99 | 1.00 |
| 1235 | 2375.0 | T, CF | 0.00 | 0.99 | 0.94 |
| 1236 | 2377.5 | T, CF, $CO_2$ | 0.00 | 0.99 | 1.00 |
| 1237 | 2380.0 | T, CF | 0.00 | 0.99 | 0.96 |
| 1238 | 2382.5 | T, CF | 0.00 | 0.90 | 1.00 |
| 1239 | 2385.0 | T, CF, $CO_2$ | 0.00 | 0.99 | 0.99 |
| 1241 | 2390.0 | T, CF | 0.08 | 0.99 | 1.00 |

**T1: The NOAA/NESDIS CrIS Channel Selection (See legend at the bottom)**

| I | $cm^{-1}$ | Chn Sensitivity | $\tau_{fix}$ | $\tau_{HO_2}$ | $\tau_{O_3}$ |
|---|---|---|---|---|---|
| 1242 | 2392.5 | T, CF, $CO_2$ | 0.20 | 0.99 | 1.0 |
| 1243 | 2395.0 | T, CF | 0.31 | 0.99 | 1.0 |
| 1244 | 2397.5 | T, CF | 0.37 | 0.99 | 1.0 |
| 1245 | 2400.0 | $CO_2$ | 0.41 | 0.99 | 1.0 |
| 1247 | 2405.0 | T, CF | 0.47 | 0.99 | 1.0 |
| 1250 | 2412.5 | T, CF | 0.52 | 0.99 | 1.0 |
| 1270 | 2462.5 | Srf | 0.76 | 0.99 | 1.0 |
| 1271 | 2465.0 | Srf | 0.77 | 0.99 | 1.0 |
| 1282 | 2492.5 | Srf | 0.86 | 0.99 | 1.0 |
| 1285 | 2500.0 | Srf | 0.89 | 0.99 | 1.0 |
| 1288 | 2507.5 | Srf | 0.90 | 0.99 | 1.0 |
| 1290 | 2512.5 | Srf | 0.90 | 0.99 | 1.0 |
| 1293 | 2520.0 | Srf | 0.92 | 0.99 | 1.0 |
| 1298 | 2532.5 | Srf | 0.90 | 0.98 | 1.0 |
| 1301 | 2540.0 | Srf | 0.87 | 0.99 | 1.0 |

## 5.1 Table legend

- column 1: frequency index
- column 2: wave number
- column 3: channel sensitivity flags:

  T: temperature sensitive channels

  Srf: Surface temperature and emissivity sensitive channels

  $H_2O$: water vapor sensitive channels

  $O_3$: ozone sensitive channels

  CF: cloud filtering channels

  CH: cloud height channels

  $CO_2$: carbon dioxide sensitive channels

  $CH_4$: methane sensitive channels

  $CO$: carbon monoxide sensitive channels

  $HNO_3$: $HNO_3$ sensitive channels

  $N_2O$: $N_2O$ sensitive channels

  $SO_2$: $SO_2$ sensitive channels
- column 4: Mid-latitude atmosphere total transmittance of fixed concentration atmospheric gases
- column 5: Mid-latitude atmosphere water vapor total transmittance
- column 6: Mid-latitude atmosphere ozone and liquid water total transmittance

## Acknowledgements

The authors wish to thank Walter Wolf for his useful suggestions on the topic of this paper, Murty Divakarla for providing the CrIS proxy data set and Eric Maddy for installing the CrIS SARTA RTA version 10a into the NOAA system.

## References

[1] C.D. Barnet, Murty Divakarla, Mitch Goldberg, Tom King, Guang Guo, and Nick Nalli. The cris/atms proxy data package for the crimss edr generation and evaluation (release 1.0), ipo report. Technical report, 2010.

[2] M. T. Chahine. Remote sounding of cloudy atmospheres in a single cloud layer. *J. Atmos. Sci.*, 31:233–243, 1974.

[3] A.D. Collard. Selection of iasi channels for use in numerical weather prediction. *QJRMS*, 133:1977–1991, 2007.

[4] CrIS. Cross-track infrared sounder. http://www.ipo.noaa.gov, 2011.

[5] B.S. Everitt. *Cambridge Dictionary of Statistics (2nd Edition)*. CUP ISBN 0-521-81099-x, 2002.

[6] A. Gambacorta. The iasi algorithm theorethical basis documentation. http://www.star.nesdis.noaa.gov/smcd/spb/iosspdt/qadocs/IASIPhase2 /IASIATBDPhaseII20111115.pdf, 2011.

[7] A. Gambacorta, C. Barnet, W.Wolf, and M.Goldberg. The noaa/nesdis near real time iasi channel selection for data assimilation and retrieval purposes. Technical report, National Oceanic and Atmospheric Administration (NOAA) NESDIS Technical Report, 2007.

[8] J.Jong, 2011. Personal communications.

[9] L. D. Kaplan. The use of high-frequency infrared radiometry for remote atmospheric probing with high vertical resolution. Technical Report MIT Publication, Department of Meteorology, Massachusetts Institute of Technology, 1969.

[10] L. D. Kaplan, M. T. Chahine, J. Susskind, and J. E. Searl. Spectral band passes for a high precision satellite sounder. *Appl. Opt.*, 16:322–325, 1977.

[11] N.Fourrie and J-N. Thepaut. Validation of the nesdis near real time airs channel selection. Technical report, European Centre for medium-Range Weather Forecasts, 2002.

[12] F. Rabier, N. Fourrie, D. Chafai, and P. Prunet. Channel selection methods for infrared atmospheric sounding interferometer radiances. Technical report, The IASI Science Plan Report, 2002.

[13] C.D. Rodgers. Information content and optimization of high spectral resolution measurements. *Proceedings of SPIE*, 2830:136–147, 1996.

[14] L. Strow and S. Hannon. Noaa implemented version v10a, 2011.

[15] J. Susskind, C. D. Barnet, and J. Blaisdell. Retrieval of atmospheric and surface parameters from AIRS/AMSU/HSB data in the presence of clouds. *IEEE Trans. Geosci. Remote Sensing*, 41(2), 2003.

**NESDIS 111** An Algorithm for Correction of Lunar Contamination in AMSU-A Data. Seiichiro Kigawa and Tsan Mo, December 2002.

**NESDIS 112** Sampling Errors of the Global Mean Sea Level Derived from Topex/Poseidon Altimetry. Chang-Kou Tai and Carl Wagner, December 2002.

**NESDIS 113** Proceedings of the International GODAR Review Meeting: Abstracts. Sponsors: Intergovernmental Oceanographic Commission, U.S. National Oceanic and Atmospheric Administration, and the European Community, May 2003.

**NESDIS 114** Satellite Rainfall Estimation Over South America: Evaluation of Two Major Events. Daniel A. Vila, Roderick A. Scofield, Robert J. Kuligowski, and J. Clay Davenport, May 2003.

**NESDIS 115** Imager and Sounder Radiance and Product Validations for the GOES-12 Science Test. Donald W. Hillger, Timothy J. Schmit, and Jamie M. Daniels, September 2003.

**NESDIS 116** Microwave Humidity Sounder Calibration Algorithm. Tsan Mo and Kenneth Jarva, October 2004.

**NESDIS 117** Building Profile Plankton Databases for Climate and EcoSystem Research. Sydney Levitus, Satoshi Sato, Catherine Maillard, Nick Mikhailov, Pat Cadwell, Harry Dooley, June 2005.

**NESDIS 118** Simultaneous Nadir Overpasses for NOAA-6 to NOAA-17 Satellites from 1980 and 2003 for the Intersatellite Calibration of Radiometers. Changyong Cao, Pubu Ciren, August 2005.

**NESDIS 119** Calibration and Validation of NOAA 18 Instruments. Fuzhong Weng and Tsan Mo, December 2005.

**NESDIS 120** The NOAA/NESDIS/ORA Windsat Calibration/Validation Collocation Database. Laurence Connor, February 2006.

**NESDIS 121** Calibration of the Advanced Microwave Sounding Unit-A Radiometer for METOP-A. Tsan Mo, August 2006.

**NESDIS 122** JCSDA Community Radiative Transfer Model (CRTM). Yong Han, Paul van Delst, Quanhua Liu, Fuzhong Weng, Banghua Yan, Russ Treadon, and John Derber, December 2005.

**NESDIS 123** Comparing Two Sets of Noisy Measurements. Lawrence E. Flynn, April 2007.

**NESDIS 124** Calibration of the Advanced Microwave Sounding Unit-A for NOAA-N'. Tsan Mo, September 2007.

**NESDIS 125** The GOES-13 Science Test: Imager and Sounder Radiance and Product Validations. Donald W. Hillger, Timothy J. Schmit, September 2007

**NESDIS 126** A QA/QC Manual of the Cooperative Summary of the Day Processing System. William E. Angel, January 2008.

**NESDIS 127** The Easter Freeze of April 2007: A Climatological Perspective and Assessment of Impacts and Services. Ray Wolf, Jay Lawrimore, April 2008.

**NESDIS 128** Influence of the ozone and water vapor on the GOES Aerosol and Smoke Product (GASP) retrieval. Hai Zhang, Raymond Hoff, Kevin McCann, Pubu Ciren, Shobha Kondragunta, and Ana Prados, May 2008.

**NESDIS 129** Calibration and Validation of NOAA-19 Instruments. Tsan Mo and Fuzhong Weng, editors, July 2009.

**NESDIS 130** Calibration of the Advanced Microwave Sounding Unit-A Radiometer for METOP-B. Tsan Mo, August 2010

**NESDIS 131** The GOES-14 Science Test: Imager and Sounder Radiance and Product Validations. Donald W. Hillger and Timothy J. Schmit, August 2010.

**NESDIS 132** Assessing Errors in Altimetric and Other Bathymetry Grids. Karen M. Marks and Walter H.F. Smith, January 2011.

## NOAA SCIENTIFIC AND TECHNICAL PUBLICATIONS

***The National Oceanic and Atmospheric Administration*** **was established as part of the Department of Commerce on October 3, 1970. The mission responsibilities of NOAA are to assess the socioeconomic impact of natural and technological changes in the environment and to monitor and predict the state of the solid Earth, the oceans and their living resources, the atmosphere, and the space environment of the Earth.**

**The major components of NOAA regularly produce various types of scientific and technical information in the following types of publications**

**PROFESSIONAL PAPERS – Important definitive research results, major techniques, and special investigations.**

**CONTRACT AND GRANT REPORTS – Reports prepared by contractors or grantees under NOAA sponsorship.**

**ATLAS – Presentation of analyzed data generally in the form of maps showing distribution of rainfall, chemical and physical conditions of oceans and atmosphere, distribution of fishes and marine mammals, ionospheric conditions, etc.**

**TECHNICAL SERVICE PUBLICATIONS – Reports containing data, observations, instructions, etc. A partial listing includes data serials; prediction and outlook periodicals; technical manuals, training papers, planning reports, and information serials; and miscellaneous technical publications.**

**TECHNICAL REPORTS – Journal quality with extensive details, mathematical developments, or data listings.**

**TECHNICAL MEMORANDUMS – Reports of preliminary, partial, or negative research or technology results, interim instructions, and the like.**

**U.S. DEPARTMENT OF COMMERCE**
**National Oceanic and Atmospheric Administration**
**National Environmental Satellite, Data, and Information Service**
**Washington, D.C. 20233**